



## Helium diffusivity in oxide nuclear fuel: Critical data analysis and new correlations



L. Luzzi<sup>a,\*</sup>, L. Cognini<sup>a,b</sup>, D. Pizzocri<sup>a</sup>, T. Barani<sup>a</sup>, G. Pastore<sup>c</sup>, A. Schubert<sup>b</sup>, T. Wiss<sup>b</sup>, P. Van Uffelen<sup>b</sup>

<sup>a</sup> Politecnico di Milano, Department of Energy, Nuclear Engineering Division, Via La Masa 34, 20156 Milan, Italy

<sup>b</sup> European Commission, Joint Research Centre, Directorate for Nuclear Safety and Security, P.O. Box 2340, 76125 Karlsruhe, Germany

<sup>c</sup> Idaho National Laboratory, Fuel Modeling and Simulation Department, 2525 Fremont Avenue, 83415 Idaho Falls, United States

### ARTICLE INFO

#### Keywords:

Inert gas behaviour  
Helium behaviour  
Diffusivity  
Oxide fuel

### ABSTRACT

Helium is relevant in determining nuclear fuel behaviour. It affects the performance of nuclear fuel both in reactor and in storage conditions. Helium becomes important in reactor conditions when high burnups are targeted or MOX fuel is used, whereas for storage conditions it can represent a threat to the fuel rods integrity. The accurate knowledge of helium behaviour combined with predictive model capabilities is fundamental for the safe management of nuclear fuel, with helium diffusivity being a critical property. For this reason, a considerable number of separate effect experiments in the last fifty years investigated helium diffusivity in nuclear fuel. The aim of this work is to critically review and assess the experimental results concerning the helium diffusivity. Experimental results are critically analysed in terms of the helium introduction technique used (either infusion, implantation or doping) and of sample characteristics (single crystal, poly-crystal or powder). Accordingly, we derived two different correlations for the diffusivity. Clearly, each of the new correlations corresponds to a limited range of application conditions, depending on the experimental data used to derive it. We provide recommendations regarding the proper application conditions for each correlation (e.g., in reactor or storage conditions).

### 1. Introduction

The knowledge of helium behaviour in nuclear fuel is of fundamental importance for its safe operation and storage (Olander, 1976; Rossiter, 2012). This is true irrespectively of the particular fuel cycle strategy adopted. In fact, both open and closed fuel cycles tend towards operating nuclear fuel to higher burnups (i.e., keeping the fuel in the reactor for a longer time to extract more specific energy from it), thus implying higher accumulation of helium in the fuel rods themselves (Rondinella et al., 2003). Moreover, considering open fuel cycles foreseeing the disposal of spent fuel, the helium production rate in the spent nuclear fuel is positively correlated with the burnup at discharge, and the production of helium (by  $\alpha$ -decay of minor actinides) progresses during storage of spent fuel (Crossland, 2012; Wiss et al., 2014). On the other hand, closed fuel cycles imply the use of fuels with higher concentrations of minor actinides (e.g., minor actinides bearing blankets, MABB), thus they are characterized by higher helium production rates during operation (Crossland, 2012).

Helium is produced in nuclear fuel by ternary fissions, ( $n,\alpha$ )-

reactions and  $\alpha$ -decay (Botazzoli, 2011; Ewing et al., 1995; Federici et al., 2007). After its production, helium precipitates into intra- and inter-granular bubbles and can be absorbed/released from/to the nuclear fuel rod free volume (Booth, 1957; Matzke, 1980). Helium can thus contribute to the fuel swelling (and eventually the stress in the cladding after mechanical contact is established), the pressure in the fuel rod free volume, and the gap conductance (giving feedback to the fuel temperature) (Piron et al., 2000).

Among the properties governing the behaviour of helium in nuclear fuel, its diffusivity and solubility govern the transport and absorption/release mechanisms (Maugeri et al., 2009; Nakajima et al., 2011; Talip et al., 2014a). Compared to xenon and krypton, helium presents both a higher solubility and diffusivity in oxide nuclear fuel (Belle, 1961; Petit et al., 2003; Rufe et al., 1965). These high values of helium solubility and diffusivity are responsible for its peculiar behaviour, characterized by phenomena that are not observed for xenon and krypton (e.g., helium absorption, helium thermal re-solution from bubbles) (Donnelly and Evans, 1991).

A considerable amount of experiments has been performed with the

\* Corresponding author.

E-mail address: [lelio.luzzi@polimi.it](mailto:lelio.luzzi@polimi.it) (L. Luzzi).

**Table 1**  
Summary of the experimental works considered in this overview.

Ref.	Sample	Technique of He introduction	He release measurement method
(Belle, 1961)	UO <sub>2</sub> powder (0.16 μm)	Infusion	Dissolution and MS <sup>a</sup>
(Rufeh, 1964)	UO <sub>2</sub> powder (4 μm)	Infusion	Dissolution and MS
(Rufeh et al., 1965)			
(Sung, 1967)	UO <sub>2</sub> single-crystal (1 μm)	Infusion	Dissolution and MS
(Trocellier et al., 2003)	UO <sub>2</sub> poly-crystal	Ion Implantation	μNRA <sup>b</sup> <sup>3</sup> He(d,p)α
(Guilbert et al., 2004)	UO <sub>2</sub> poly-crystal (8 μm)	Ion Implantation	NRA <sup>3</sup> He(d,α)H
		Fluence <sup>3</sup> He (m <sup>-2</sup> ) = 10 <sup>20</sup>	
(Roudil et al., 2004)	UO <sub>2</sub> poly-crystal (10 μm)	Ion Implantation	NRA <sup>3</sup> He(d,p)α
		Fluence <sup>3</sup> He (m <sup>-2</sup> ) = 0.3·10 <sup>20</sup>	
		Fluence <sup>3</sup> He (m <sup>-2</sup> ) = 3·10 <sup>20</sup>	
(Ronchi and Hiernaut, 2004)	(U <sub>0.9</sub> , <sup>238</sup> Pu <sub>0.1</sub> ) O <sub>2</sub> poly-crystal	Doping	KEMS
(Martin et al., 2006)	UO <sub>2</sub> poly-crystal (24 μm)	Ion Implantation	NRA <sup>3</sup> He(d,α)H
		Fluence <sup>3</sup> He (m <sup>-2</sup> ) = (1.7 ± 0.06)·10 <sup>20</sup>	
(Pipon et al., 2009)	(U <sub>0.75</sub> , <sup>239</sup> Pu <sub>0.25</sub> ) O <sub>2</sub> poly-crystal	Ion Implantation	NRA <sup>3</sup> He(d,p)α
		Fluence <sup>3</sup> He (m <sup>-2</sup> ) = 5·10 <sup>19</sup>	
(Nakajima et al., 2011)	UO <sub>2</sub> single-crystal (18 μm)	Infusion	KEMS
(Garcia et al., 2012)	UO <sub>2</sub> poly-crystal	Ion Implantation	NRA <sup>3</sup> He(d,α)H
		Fluence <sup>3</sup> He (m <sup>-2</sup> ) = 10 <sup>20</sup>	
(Talip et al., 2014a)	(U <sub>0.999</sub> , <sup>238</sup> Pu <sub>0.001</sub> ) O <sub>2</sub> poly-crystal (10 μm)	Doping	KEMS

<sup>a</sup> Mass Spectrometry.

<sup>b</sup> NRA (Nuclear Reaction Analysis) is a nuclear method to obtain the profile of helium implanted in samples, using <sup>3</sup>He(d,p)α and <sup>3</sup>He(d,α)H reactions (Martin et al., 2006; Pipon et al., 2009).

goal of determining the diffusivity and solubility of helium in nuclear fuel (Belle, 1961; Garcia et al., 2012; Guilbert et al., 2004; Hasko and Swarc, 1963; Martin et al., 2006; Maugeri et al., 2009; Nakajima et al., 2011; Pipon et al., 2009; Ronchi and Hiernaut, 2004; Roudil et al., 2004; Rufeh, 1964; Sung, 1967; Talip et al., 2014a; Trocellier et al., 2003). In particular, several measurements have been made to determine the helium diffusivity as a function of temperature (Belle, 1961; Garcia et al., 2012; Guilbert et al., 2004; Martin et al., 2006; Nakajima et al., 2011; Pipon et al., 2009; Ronchi and Hiernaut, 2004; Roudil et al., 2004; Rufeh, 1964; Sung, 1967; Talip et al., 2014a; Trocellier et al., 2003), whereas few experiments are available to characterise Henry's constant,<sup>1</sup>(Belle, 1961; Blanpain et al., 2006; Hasko and Swarc, 1963; Maugeri et al., 2009; Nakajima et al., 2011; Rufeh, 1964; Sung, 1967; Talip et al., 2014a).

The experimental procedures available for measuring helium diffusivity differ mainly in the way in which the helium is introduced in the fuel samples. In particular, three introduction techniques are used: (i) infusion (Belle, 1961; Nakajima et al., 2011; Rufeh, 1964; Sung, 1967; Maugeri et al., 2009), in which the sample is kept in a pressurized helium atmosphere for a certain infusion time, (ii) ionic implantation (Garcia et al., 2012; Guilbert et al., 2004; Martin et al., 2006; Pipon et al., 2009; Roudil et al., 2004; Trocellier et al., 2003), in which a beam of <sup>3</sup>He<sup>+</sup> hits and penetrates the sample, and (iii) doping (Ronchi and Hiernaut, 2004; Talip et al., 2014a), in which α-decaying elements are introduced in the sample, resulting in an internal source of helium. These introduction techniques generate different helium distributions in the samples and induce different levels of damage to the crystal lattice of the sample (Labrim et al., 2007; Talip et al., 2014a). Depending on the introduction technique used, different measuring techniques are adopted to determine the concentration of helium introduced in the sample. A relation is then established between the helium concentration and the diffusivity (Rufeh, 1964; Sung, 1967).

Moreover, helium diffusivity has been measured for samples with different microstructures, i.e., single crystals, poly-crystals, and powders.

In the light of the profound differences in experimental techniques and in microstructure of the samples, the correlations derived from rough data fitting must be critically analysed. In fact, the spread of

available diffusivities is extremely large. Nevertheless, currently used correlations for the helium diffusivity are still derived from rough data fitting (Garcia et al., 2012; Nakajima et al., 2011; Ronchi and Hiernaut, 2004; Roudil et al., 2004; Talip et al., 2014a) or are intended to be upper/lower boundaries enveloping the data (Federici et al., 2007; Ronchi and Hiernaut, 2004).

In this work, we provide a complete overview of all the experimental results obtained for helium diffusivity in oxide nuclear fuel. The experimental results are classified according to the helium introduction technique used. At last, we derive empirical correlations and recommend the most suitable values of the helium diffusivity in the main cases of interest (e.g., in-pile, storage or annealing condition). The derivation of empirical correlations is complemented by an uncertainty analysis.

## 2. Review of experimental results

Early measurements of the helium diffusivity in oxide nuclear fuel have been performed since the 1960s. The growing interest in determining helium behaviour in nuclear fuel to assess its performance in storage conditions translated in several new experiments performed in the last twenty years. In this Section, we give an overview of all the experimental results available in the open literature, organized in chronological order, as reported in Table 1.

Helium can be introduced into oxide nuclear fuel samples by infusion (Nakajima et al., 2011; Rufeh et al., 1965; Sung, 1967), ion implantation (Garcia et al., 2012; Guilbert et al., 2004; Martin et al., 2006; Pipon et al., 2009; Roudil et al., 2004; Trocellier et al., 2003) or by doping the matrix with short-lived α-emitters (Ronchi and Hiernaut, 2004; Talip et al., 2014a). Fig. 1 shows a sketch of the different experimental techniques herein considered. Depending on the helium introduction technique, the crystalline lattice suffers different levels of damage. Crystalline lattices with different damage levels show different helium behaviour. Moreover, each technique used to introduce the helium in the sample has a corresponding specific technique to measure the amount of helium introduced.

Belle (1961) first studied the diffusivity of helium in a UO<sub>2</sub> powder. After his work, the helium diffusivity in oxide nuclear fuels was estimated by Rufeh (Rufeh et al., 1965; Rufeh, 1964) and Sung (1967) using UO<sub>2</sub> samples (some in powder form and some single crystal) with helium introduced through the infusion technique.

<sup>1</sup> Early work from (Rufeh, 1964; Sung, 1967) demonstrated the validity of Henry's law for the system helium/oxide fuel.

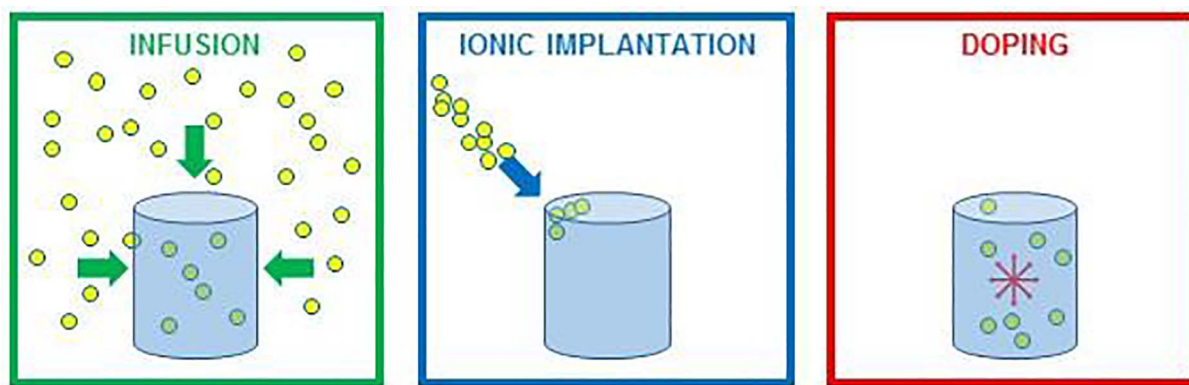


Fig. 1. Sketch of the different experimental techniques used to introduce helium in nuclear fuel samples.

In a more recent study, Trocellier et al. (2003) measured the thermal diffusivity of  $^3\text{He}$  implanted in different nuclear materials. Subsequently, also Guilbert et al. (2004) and Roudil et al. (2004) performed similar experiments in similar temperature ranges (around 1173–1373 K), both using samples of polycrystalline  $\text{UO}_2$ . In particular, Roudil et al. (2004) used two values of  $^3\text{He}$  fluence, showing that helium diffusivity is higher for lower implantation fluences. They ascribed this behaviour to helium trapping at defects sites. Ronchi and Hiernaut (2004) focused their activity on the mixed oxide fuel ( $\text{U}_{0.9}, ^{238}\text{Pu}_{0.1}\text{O}_2$ ), exploiting the plutonium content as a doping of the sample itself ( $^{238}\text{Pu}$  is a short-lived, hence convenient  $\alpha$ -emitter). This was the first experimental work about helium diffusivity in mixed oxide fuel. Martin et al. (2006) measured helium concentrations in disks of polycrystalline  $\text{UO}_2$ , using the implantation technique. Pipon et al. (2009) applied the implantation technique to determine the diffusivity of mixed oxide samples with stoichiometry ( $\text{U}_{0.75}, ^{239}\text{Pu}_{0.25}\text{O}_2$ ).

Furthermore, Nakajima et al. (2011) determined the helium diffusivity in single crystal  $\text{UO}_2$  samples. They adopted the infusion technique and measured the helium infused concentration through a Knudsen–effusion mass-spectrometric method (KEMS)<sup>2</sup>. Garcia et al. (2012) measured the helium diffusivity in samples of polycrystalline  $\text{UO}_2$  implanted at a fluence of  $10^{20} \text{ } ^3\text{He}\cdot\text{m}^{-2}$ . They also estimated the diffusivity of helium at grain boundaries by comparing their results to those obtained from single-crystal samples. Talip et al. (2014a) used  $^{238}\text{Pu}$ -doped  $\text{UO}_2$  samples. They measured the helium release rate as a function of the annealing temperature and used this information to derive the diffusivity of helium single atoms and of helium bubbles as well (Talip et al., 2014a). Moreover, this study leveraged on the TEM technique, employed to obtain images of the sample before and after the introduction of helium. TEM provides additional qualitative and quantitative information, which is very useful for the modelling and interpretation of the outcome of the experiment (e.g., the amount of helium that precipitates into bubbles, the size of these bubbles and their location) (Talip et al., 2014a).

A recent study by Talip et al. (2014b) investigated the diffusivity of helium in non-stoichiometric  $\text{UO}_2$  fuel samples. This is of major interest because the fuel gradually transitions into a hyper-stoichiometric composition during storage (Wiss et al., 2014), and during operation if high burnups are achieved (Lewis et al., 2012) or clad failure occurs. The results of this work indicated that the diffusivity of helium is higher in non-stoichiometric samples compared to the diffusivity in stoichiometric ones, for both single crystals and polycrystalline microstructures (Crocombette, 2002), which is in line with the findings for Xe by Matzke (1980).

In conclusion of this brief overview, it is worth mentioning the

important contribution to these studies arising from molecular dynamics (MD) calculations (Martin et al., 2006; Yakub et al., 2010). In particular, Yakub et al. (2010) investigated both hypo- and hyper-stoichiometric  $\text{UO}_2$ . They concluded that small deviations from stoichiometry significantly accelerated helium diffusion, in agreement with the experimental results for hyper-stoichiometric samples (Yakub et al., 2009). Yakub suggests that non-stoichiometry increases helium diffusivity because it provides more paths for the movement of helium atoms within the lattice. The strength of this effect appears to be more pronounced in the hypo-stoichiometric domain (Govers et al., 2009; Yakub et al., 2010).

In the following subsections, we describe the experimental results briefly introduced above. We categorize them depending on the technique used to introduce the helium in the sample. This is motivated by different techniques causing different levels of damage in the crystal lattice of the sample, which may affect the diffusivity of helium in the sample itself (Talip et al., 2014b). Furthermore, for each experimental result, we specify the sample microstructure.

Clearly, several other crucial aspects could contribute in explaining the spread observed in the experimental data (e.g., the specific conditions/atmospheres of the annealing experiments, the evolution of lattice damage during annealing, the potential trapping of helium atoms at defects sites, ...). Nevertheless, very limited experimental information is available to enlighten these effects. We therefore decided to keep an engineering approach and proceed with a categorization based only on the technique used to introduce the helium in the sample.

### 2.1. Infusion

As mentioned above, there are four experimental studies in which the infusion technique was used to introduce helium in samples (Belle, 1961; Nakajima et al., 2011; Rufeh, 1964; Sung, 1967). The results of these experiments in terms of diffusivity are collected in Table 2 and plotted in Fig. 2.

The experimental results obtained via the infusion technique cover a wide range of temperatures, from 968 K to 2110 K. The spread of the diffusivities is of one-two (1-2) orders of magnitude (Fig. 2). This experimental spread is in line with the spread of the diffusivities of other inert gases (i.e., xenon and krypton) (Matzke, 1980).

No clear dependence of the data upon the crystalline structure of the samples (either single crystals or powders) is observable (Fig. 2).

### 2.2. Implantation

Several recent experimental studies used the ion implantation technique to introduce the helium in samples (Garcia et al., 2012; Guilbert et al., 2004; Martin et al., 2006; Pipon et al., 2009; Roudil et al., 2004; Trocellier et al., 2003). The results of these experiments in

<sup>2</sup> KEMS is a method to determine the quantity of helium released during thermal desorption (Colle et al., 2014, 2013; Talip et al., 2014a).

**Table 2**  
Summary of the experimental helium diffusivities in oxide fuel obtained via the infusion technique.

Ref.	Sample	Diffusivity ( $\text{m}^2 \text{s}^{-1}$ ) <sup>a</sup>	Temperature (K)
Belle (1961)	UO <sub>2</sub> powder (0.16 $\mu\text{m}$ )	$9.05 \cdot 10^{-22}$	968
		$1.01 \cdot 10^{-20}$	1070
		$4.08 \cdot 10^{-20}$	1166
		$1.86 \cdot 10^{-19}$	1268
Rufeh (1964) Rufeh et al. (1965)	UO <sub>2</sub> powder (4 $\mu\text{m}$ )	$1.5 \cdot 10^{-17}$	1473
Sung (1967)	UO <sub>2</sub> single crystal (1 $\mu\text{m}$ )	$6.14 \cdot 10^{-18}$	1473
		$9.15 \cdot 10^{-18}$	1623
		$12.57 \cdot 10^{-18}$	1773
Nakajima et al. (2011) <sup>b</sup>	UO <sub>2</sub> single crystal (18 $\mu\text{m}$ )	$9.50 \cdot 10^{-10} \exp[-2.05/kT]$	Range: 1170–2110
		$4.88 \cdot 10^{-10} \exp[-1.93/kT]$	Range: 1390–2070

<sup>a</sup> The activation energy is expressed in electronvolt (eV). The Boltzmann constant,  $k$ , is coherently expressed in  $\text{eV K}^{-1}$ .

<sup>b</sup> The annealing of the samples has been performed with the KEMS method (Colle et al., 2014, 2013; Talip et al., 2014a).

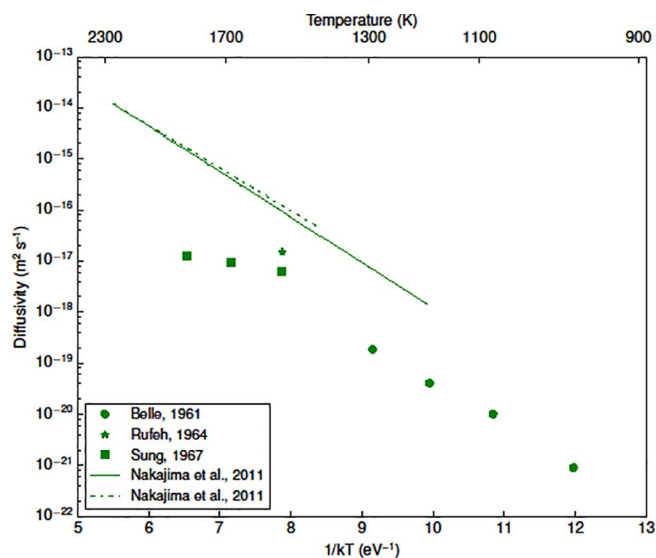


Fig. 2. Plot of the experimental helium diffusivity in oxide fuel obtained via the infusion technique, as a function of temperature.

terms of diffusivity are collected in Table 3 and plotted in Fig. 3.

The experimental results obtained via the ion implantation technique cover a rather limited range of temperatures compared to those derived via the infusion technique (from 968 K to 2110 K for the infused and from 973 K to 1373 K for the implanted, respectively). The spread of the diffusivities is around three (3) orders of magnitude. Again, this experimental spread is in line with the spread of the diffusivities of other inert gases (i.e., xenon and krypton) (Matzke, 1980).

All the samples used in these experiments are poly-crystals. Hence, it is impossible to attempt a categorization of the available diffusivities in terms of microstructure.

### 2.3. Doping

Only two experimental studies used the doping technique to introduce the helium in samples (Ronchi and Hiernaut, 2004; Talip et al., 2014a). The results of these experiments in terms of diffusivity are collected in Table 4 and plotted in Fig. 4.

The experimental results obtained via the doping cover the range of temperature from 1320 K to 1800 K (Talip et al., 2014a), whereas the range for the results of Ronchi and Hiernaut (Ronchi and Hiernaut, 2004) is not specified. The spread of the data is of three-four (3–4)

orders of magnitude and may be influenced by the large difference in damage accumulation (displacements per atom). Again, this experimental spread is in line with the spread of the diffusivities of other inert gases (i.e., xenon and krypton) (Matzke, 1980).

### 3. Derivation of empirical correlations

The experimental diffusivities are categorized depending on the technique used to introduce the helium in the samples. With this categorization, two clusters of data become evident: the measurements performed via the infusion technique are in the lower region of the diffusivity range, whereas the measurements performed via the ion implantation and doping techniques lie in the upper region (Fig. 5). We ascribe this major clustering of the data to the different level of lattice damage induced by the different experimental techniques used to introduce helium in the samples. In particular, ion implantation and doping introduce additional defects in the crystal lattice of the sample (Talip et al., 2014b), enhancing diffusion. This conclusion is in line with the studies showing enhanced diffusion in hypo- and hyper-stoichiometric samples (Talip et al., 2014b; Yakub et al., 2010), i.e., in samples characterized by somewhat altered crystal lattices.

Considering the two clusters, we propose two distinct empirical correlations for the helium diffusivity: one based on the data for infused samples and another one based on the data for implanted and doped samples. This implies that one correlation is suited for applications with no (or very limited) lattice damage, whereas the other is more suited for applications with significant lattice damage,<sup>3</sup> which is consistent with the difference observed between the two sets of data obtained with the doping technique.

The proposed correlations are in the form  $D = D_0 \exp[-Q/kT]$ . Available data do not support the inclusion of other regressors besides temperature (e.g., only two data include plutonium concentration and each cluster includes only up to two microstructures).

Table 5 collects the derived fitting parameters and the uncertainties related to each fitting parameter and to the diffusivity prediction as well.<sup>4</sup> We can notice that the parameters for the correlation for ion implantation and doping data is affected by high

<sup>3</sup> The statement that each correlation herein derived should be applied in different situations depending on the lattice damage is meant as an indication, and not as a general conclusion. In fact, it is difficult to derive strong conclusions considering the limited numbers of available data. Nevertheless, this indication appears to be supported by the available data (within the temperature range covered by the available data).

<sup>4</sup> For those experimental data that were given already in the form of a line, we included in the fit only the points at the extremes of the temperature range as representative of the two degrees of freedom of the line.

**Table 3**  
Summary of the experimental helium diffusivities in oxide and mixed oxide fuel obtained via the ion implantation technique.

Ref.	Sample	Diffusivity (m <sup>2</sup> s <sup>-1</sup> ) <sup>a</sup>	Temperature (K)
Trocélier et al. (2003)	UO <sub>2</sub> poly-crystal	(3.7 ± 0.74)·10 <sup>-18</sup>	1273
Guilbert et al. (2004)	UO <sub>2</sub> poly-crystal (8 μm)	6·10 <sup>-17</sup>	1373
Roudil et al. (2004)	UO <sub>2</sub> poly-crystal (10 μm)	8·10 <sup>-9</sup> exp[-(2 ± 0.1)/kT] <sup>b</sup> 4·10 <sup>-10</sup> exp[-(2 ± 0.1)/kT] <sup>c</sup>	Range: 1123–1273 Range: 1123–1273
Martin et al. (2006)	UO <sub>2</sub> poly-crystal (24 μm)	2.25·10 <sup>-17</sup> 7.6·10 <sup>-17</sup>	1073 1373
Pipon et al. (2009) <sup>d</sup>	(U <sub>0.75</sub> , <sup>239</sup> Pu <sub>0.25</sub> )O <sub>2</sub> poly-crystal	9.2·10 <sup>-18</sup> 1.6·10 <sup>-16</sup>	1123 1273
Garcia et al. (2012)	UO <sub>2</sub> poly-crystal	5·10 <sup>-10</sup> exp[-(1.4 ± 0.2)/kT]	Range: 973–1373

<sup>a</sup> The activation energy is expressed in electronvolt (eV). The Boltzmann constant, *k*, is coherently expressed in eV K<sup>-1</sup>.  
<sup>b</sup> This result is derived from a sample implanted with a helium fluence of 0.3·10<sup>20</sup> m<sup>-2</sup> (Roudil et al., 2004).  
<sup>c</sup> This result is derived from a sample implanted with a helium fluence of 3·10<sup>20</sup> m<sup>-2</sup> (Roudil et al., 2004).  
<sup>d</sup> The samples used by Pipon et al. are made of UO<sub>2</sub> pellets with 24.5 wt% of plutonium (mainly <sup>239</sup>Pu) (Pipon et al., 2009).

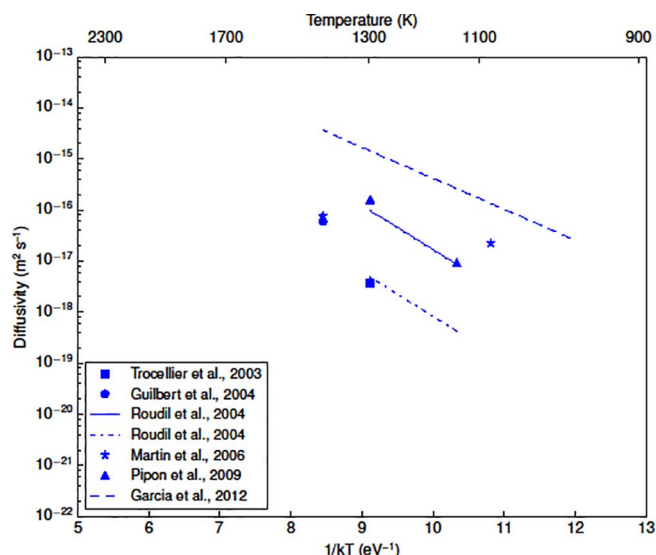


Fig. 3. Plot of the experimental helium diffusivity in oxide fuel obtained via the ion implantation technique, as a function of temperature.

uncertainty, related to the wide spread of the experimental data. Every comparison between the two correlations, in terms of activation energy *Q* and pre-exponential factor *D*<sub>0</sub>, represents an indication of a tendency. In fact, the available data are not sufficient to statistically support conclusions. On the other hand, since we included all the

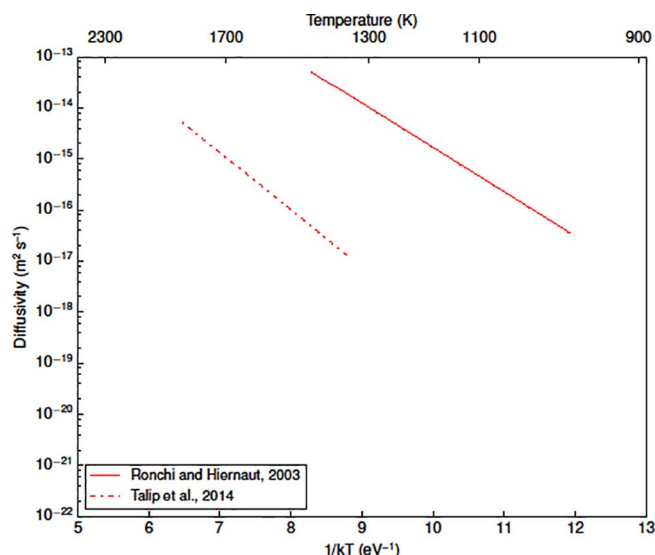


Fig. 4. Plot of the experimental helium diffusivity in oxide fuel obtained via the doping technique, as a function of temperature.

available data in the fitting procedure, these correlations are the best available at this time.

By fitting separately the two clusters of data (i.e., data from samples with no or very limited lattice damage and with significant lattice damage, respectively), we obtain an improved fitting quality. In fact, if

**Table 4**  
Summary of the experimental helium diffusivities in oxide and mixed oxide fuel obtained via the doping technique.

Ref.	Sample	Diffusivity (m <sup>2</sup> s <sup>-1</sup> ) <sup>a</sup>	Temperature (K)	dpa <sup>b</sup>
Ronchi and Hiernaut (2004)	(U <sub>0.9</sub> , <sup>238</sup> Pu <sub>0.1</sub> )O <sub>2</sub> poly-crystal	(8 ± 2)·10 <sup>-7</sup> exp[-(2.00 ± 0.02)/kT]	N/A	0.7 <sup>c</sup>
Talip et al. (2014a) <sup>d</sup>	(U <sub>0.999</sub> , <sup>238</sup> Pu <sub>0.001</sub> )O <sub>2</sub> poly-crystal (10 μm)	10 <sup>-7</sup> exp[-2.59/kT]	Range: 1320–1800	0.04

<sup>a</sup> The activation energy is expressed in electronvolt (eV). The Boltzmann constant, *k*, is coherently expressed in eV K<sup>-1</sup>.  
<sup>b</sup> Displacement per atom (dpa).  
<sup>c</sup> As reported by Talip et al. (2014a).  
<sup>d</sup> Talip et al. also proposed a diffusivity for helium bubbles in the same temperature range, equal to 10<sup>-10</sup> exp[-1.9/kT] (Talip et al., 2014a).

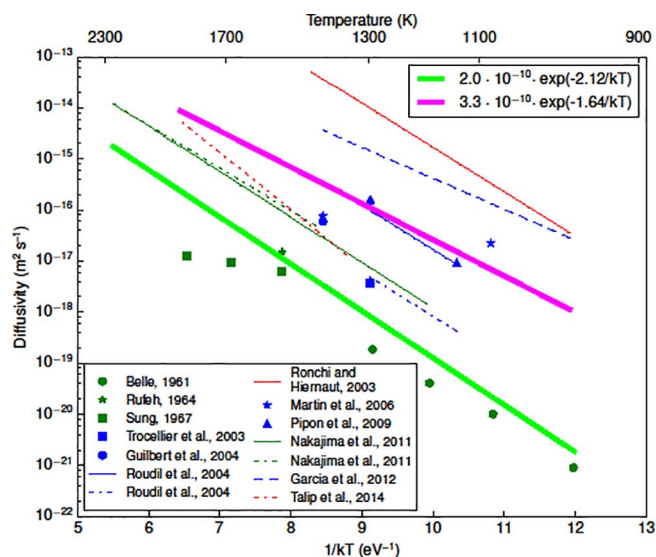


Fig. 5. Plot of the experimental helium diffusivity in oxide fuel. The measurements performed via the infusion technique (green) are clustered in the lower part of the plot, whereas in the upper part emerges a cluster of those measurements performed via the ion implantation (blue) and doping (red) technique. This clustering is ascribed to the different level of lattice damage caused to the sample by the different experimental techniques. Each cluster is fitted by a distinct correlation (magenta and light green). (For interpretation of the references to colour in this figure legend, the reader is referred to the web version of this article.)

data clustering is disregarded, the fit of all the data has a coefficient of determination of the linear regression  $R^2 = 0.43$ .

The best estimate correlation for the cluster of data with no or very limited lattice damage is

$$D = 2.0 \cdot 10^{-10} \exp[-2.12/kT] \tag{1}$$

whereas for the cluster of data with significant lattice damage we get

$$D = 3.3 \cdot 10^{-10} \exp[-1.64/kT] \tag{2}$$

We calculated the uncertainty on the prediction of the diffusivity by propagating the uncertainty of each fitting parameter. The resulting uncertainty is of the order of a factor of ten ( $\times 10$ ) for the correlation relative to no or very limited lattice damage (Eq. (1)) and of a factor of one thousand ( $\times 1000$ ) for the correlation relative to significant lattice damage (Eq. (2)). For comparison, the uncertainty of the fit made with all the data is a factor of ten thousands ( $\times 10,000$ ). The proposed categorization therefore allows for a reduction of uncertainties of a factor of one thousand/ten, respectively.

Table 5

Summary of the information concerning the fit of correlations. The form is  $\text{Log } D = \text{Log } D_0 - Q/kT \text{ Log } e$ . For each fitting parameter, we report in round brackets the confidence intervals at 95% confidence level.

Data (Ref.)	Log $D_0$ ( $\text{m}^2 \text{s}^{-1}$ )	$Q$ (eV) <sup>a</sup>	Range (K)	$R^2$
<i>Infusion</i> (Belle, 1961; Nakajima et al., 2011; Rufeh et al. 1965; Rufeh, 1964; Sung, 1967)	-9.7 (-11, -8.4)	2.12 (1.77, 2.56)	968–2110	0.93
<i>Ion implantation and doping</i> (Garcia et al., 2012; Guilbert et al., 2004; Martin et al., 2006; Pipon et al., 2009; Roudil et al., 2004; Trocellier et al., 2003) (Ronchi and Hiernaut, 2004; Talip et al., 2014a)	-9.5 (-13, -5.8)	1.64 (0.74, 2.56)	973–1800	0.52 <sup>b</sup>

<sup>a</sup> The corresponding values of the activation energy  $Q$  (J) are  $3.4 \cdot 10^{-17}$  and  $2.6 \cdot 10^{-17}$ , respectively.

<sup>b</sup> This value of  $R^2$  does not seem fully satisfactory. Nevertheless, we still choose to report this fit since it includes all the data available in the literature. Further refinement of this correlation is of major interest, once more data will become available.

Fig. 5 collects the experimental results shown in Figs. 2–4, together with the derived correlations for each data cluster. The overall range of temperature covered by the available data is 968–2110 K.

#### 4. Conclusions and recommendations

In this work, we reviewed all the experimental results describing the helium diffusivity in oxide nuclear fuels. This is a key parameter in assessing the behaviour of nuclear fuel both in reactor and storage conditions, irrespectively of the particular fuel cycle strategy adopted.

We categorized the available experimental data for the helium diffusivity in two groups, depending on the level of damage induced in the lattice of the sample by the experimental technique used. The resulting clustering of the data motivated the derivation of two distinct correlations for the helium diffusivity as a function of temperature. These correlations have an uncertainty of a factor of ten (10) to one thousand (1000) smaller compared to the correlation obtained by statistically fitting all the data (with no critical assessment of the effect of the experimental technique). The foreseen adoption of these new correlations in integral fuel performance codes will lay the foundations for a more accurate predictive modelling of helium behaviour in nuclear fuel.

We recommend the correlation derived from data obtained by the ion implantation and doping technique in calculations for reactor and storage conditions. In fact, these experimental techniques introduce a certain level of lattice damage in the sample, which is similar to that suffered by the fuel in reactor and storage conditions. On the other hand, we recommend the use of the correlation derived from data obtained by infusion for calculations for fresh nuclear fuel.

An important conclusion of this work is the need for new experimental data, with well characterized temperature and damage levels (dose, concentration of doping elements or deviation from stoichiometry). In particular, the correlation derived herein recommended for reactor and storage conditions (presumably the most important applications) is affected by uncertainties of three (3) orders of magnitude. Since for its derivation we included all the available experimental data, new experiments are required to reduce the uncertainty associated with this correlation. If justified by reduced uncertainties, one could consider developing a further improved correlation for helium diffusivity also depending on the local fuel burnup. A further refinement will have to be performed on the basis of data obtained from damaged samples, since the magnitude and concentration of defects also affects the helium diffusivity as revealed in Table 4.

The complete characterization of helium behaviour in nuclear fuel requires the investigation of other properties besides its diffusivity. In particular, reliable correlations for helium solubility should be developed as more data become available.

## Acknowledgments

This work was supported by the GENTLE Project at the Directorate for Nuclear Safety and Security (JRC-Karlsruhe, Germany) under grant agreement No 198236, and has received funding from the Euratom research and training programme 2014–2018 through the INSPYRE project under grant agreement No 754329. This research contributes to the Joint Programme on Nuclear Materials (JPNM) of the European Energy Research Alliance (EERA), in the specific framework of the COMBATFUEL Project. The work is also part of the R&D activities carried out by Politecnico di Milano in the framework of the IAEA Coordinated Research Programme FUMAC (CRP-T12028, Fuel modelling in accident conditions).

The submitted manuscript has been authored by a contractor of the U.S. Government under Contract DE-AC07-05ID14517. Accordingly, the U.S. Government retains a non-exclusive, royalty free license to publish or reproduce the published form of this contribution, or allow others to do so, for U.S. Government purposes.

## References

- Belle, J., 1961. Uranium Dioxide: properties and nuclear applications. Library (Lond).  
 Blanpain, P., Lippens, M., Schut, H., Federov, A.V., Bakker, K., 2006. The HARLEM Project, Helium solubility in  $\text{UO}_2$ . Work. MMSNF-5, Nice, Fr.  
 Booth, A.H., 1957. A method of calculating fission gas diffusion from  $\text{UO}_2$  fuel and its application to the X-2-f loop test. At. Energy Canada Ltd. Chalk River Proj. Res. Dev. Rep. AECL-496, pp. 1–23.  
 Botazzoli, P., 2011. Helium Production and Behaviour in LWR Oxide Nuclear Fuels (Ph.D. Thesis). Politec. di Milano, Italy.  
 Colle, J.-Y., Freis, D., Benes, O., Konings, R.J.M., 2013. Knudsen effusion mass spectrometry of nuclear materials: applications and developments. ECS Trans. 46, 23–38. <http://dx.doi.org/10.1149/04601.0023ecst>.  
 Colle, J.-Y., Maugeri, E.A., Thiriet, C., Talip, Z., Capone, F., Hiernaut, J.-P., Konings, R.J.M., Wiss, T., 2014. A mass spectrometry method for quantitative and kinetic analysis of gas release from nuclear materials and its application to helium desorption from  $\text{UO}_2$  and fission gas release from irradiated fuel. J. Nucl. Sci. Technol. 51, 700–711.  
 Crocombette, J.-P., 2002. Ab initio energetics of some fission products (Kr, I, Cs, Sr and He) in uranium dioxide. J. Nucl. Mater. 305, 29–36. [http://dx.doi.org/10.1016/S0022-3115\(02\)00907-8](http://dx.doi.org/10.1016/S0022-3115(02)00907-8).  
 Crossland, I., 2012. Nuclear fuel cycle science and engineering. Woodhead Publishing Limited.  
 Donnelly, S.E., Evans, J.H., 1991. Fundamental aspects of inert gases in solids.  
 Ewing, R.C., Weber, W.J., Clinard, F.W., 1995. Radiation effects in nuclear waste forms for high-level radioactive waste. Prog. Nucl. Energy 29, 63–127. [http://dx.doi.org/10.1016/0149-1970\(94\)00016-Y](http://dx.doi.org/10.1016/0149-1970(94)00016-Y).  
 Federici, E., Courcelle, A., Blanpain, P., Cognon, H., 2007. Helium production and behavior in nuclear oxide fuels during irradiation in LWR. Proc. Int. LWR Fuel Perform. Meet. San Fr. Calif., pp. 664–673.  
 Garcia, P., Martin, G., Desgardin, P., Carlot, G., Sauvage, T., Sabathier, C., Castellier, E., Khodja, H., Barthe, M.F., 2012. A study of helium mobility in polycrystalline uranium dioxide. J. Nucl. Mater. 430, 156–165. <http://dx.doi.org/10.1016/j.jnucmat.2012.06.001>.  
 Govers, K., Lemehov, S., Hou, M., Verwerf, M., 2009. Molecular dynamics simulation of helium and oxygen diffusion in  $\text{UO}_2 \pm x$ . J. Nucl. Mater. 395, 131–139. <http://dx.doi.org/10.1016/j.jnucmat.2009.10.043>.  
 Guilbert, S., Sauvage, T., Garcia, P., Carlot, G., Barthe, M.F., Desgardin, P., Blondiaux, G., Corbel, C., Piron, J.P., Gras, J.M., 2004. He migration in implanted  $\text{UO}_2$  sintered disks. J. Nucl. Mater. 327, 88–96. <http://dx.doi.org/10.1016/j.jnucmat.2004.01.024>.  
 Hasko, S., Szwarc, R., 1963. Noble gas solubility and diffusion in  $\text{UO}_2$ . AEC, Div. React. Dev. Washing. D.C.  
 Labrim, H., Barthe, M.F., Desgardin, P., Sauvage, T., Corbel, C., Blondiaux, G., Piron, J.P., 2007. Thermal evolution of the vacancy defects distribution in 1 MeV helium implanted sintered  $\text{UO}_2$ . Nucl. Instrum. Methods Phys. Res. Sect. B Beam Interact. Mater. Atoms 261, 883–887. <http://dx.doi.org/10.1016/j.nimb.2007.04.059>.  
 Lewis, B.J., Thompson, W.T., Iglesias, F.C., 2012. Fission product chemistry in oxide fuels. In: Konings, R.J.M. (Ed.), Comprehensive Nuclear Materials. Elsevier Inc., pp. 515–546. <http://dx.doi.org/10.1016/B978-0-08-056033-5.00042-2>.  
 Martin, G., Garcia, P., Labrim, H., Sauvage, T., Carlot, G., Desgardin, P., Barthe, M.F., Piron, J.P., 2006. A NRA study of temperature and heavy ion irradiation effects on helium migration in sintered uranium dioxide. J. Nucl. Mater. 357, 198–205. <http://dx.doi.org/10.1016/j.jnucmat.2006.06.021>.  
 Matzke, H., 1980. Gas release mechanisms in  $\text{UO}_2$  – a critical review. Radiat. Eff. 53, 219–242.  
 Maugeri, E., Wiss, T., Hiernaut, J.P., Desai, K., Thiriet, C., Rondinella, V.V., Colle, J.Y., Konings, R.J.M., 2009. Helium solubility and behaviour in uranium dioxide. J. Nucl. Mater. 385, 461–466. <http://dx.doi.org/10.1016/j.jnucmat.2008.12.033>.  
 Nakajima, K., Serizawa, H., Shirasu, N., Haga, Y., Arai, Y., 2011. The solubility and diffusion coefficient of helium in uranium dioxide. J. Nucl. Mater. 419, 272–280. <http://dx.doi.org/10.1016/j.jnucmat.2011.08.045>.  
 Olander, D.R., 1976. In: Fundamental Aspects of Nuclear Reactor Fuel Elements, [http://dx.doi.org/10.1016/0022-3115\(77\)90226-4](http://dx.doi.org/10.1016/0022-3115(77)90226-4).  
 Petit, T., Freyss, M., Garcia, P., Martin, P., Ripert, M., Crocombette, J.P., Jollet, F., 2003. Molecular modelling of transmutation fuels and targets. J. Nucl. Mater. 320, 133–137. [http://dx.doi.org/10.1016/S0022-3115\(03\)00179-X](http://dx.doi.org/10.1016/S0022-3115(03)00179-X).  
 Pipon, Y., Raepsaet, C., Roudil, D., Khodja, H., 2009. The use of NRA to study thermal diffusion of helium in (U, Pu) $\text{O}_2$ . Nucl. Instrum. Methods 267, 2250–2254. <http://dx.doi.org/10.1016/j.nimb.2009.03.025>.  
 Piron, J.P., Pelletier, M., Pavageau, J., 2000. Fission Gas Behaviour in Water Reactor Fuels. OECD/NEA.  
 Ronchi, C., Hiernaut, J.P., 2004. Helium diffusion in uranium and plutonium oxides. J. Nucl. Mater. 325, 1–12. <http://dx.doi.org/10.1016/j.jnucmat.2003.10.006>.  
 Rondinella, V.V., Wiss, T., Cobos, J., Hiernaut, H., 2003. Studies on spent fuel alterations during storage and radiolysis effects on corrosion behaviour using alpha-doped  $\text{UO}_2$ , in: 9<sup>th</sup> Conference on Radioactive Waste Management and Environmental Remediation. p. 4593.  
 Rossier, G., 2012. Understanding and modelling fuel behaviour under irradiation. In: Nuclear Fuel Cycle Science and Engineering. Woodhead Publishing Limited, pp. 396–426.  
 Roudil, D., Deschanel, X., Trocellier, P., Jégou, C., Peugot, S., Bart, J.M., 2004. Helium thermal diffusion in a uranium dioxide matrix. J. Nucl. Mater. 325, 148–158. <http://dx.doi.org/10.1016/j.jnucmat.2003.11.012>.  
 Ruffe, F., Olander, D.R., Pigford, T.H., 1965. The solubility of helium in uranium dioxide. Nucl. Sci. Eng.  
 Ruffe, F., 1964. Solubility of Helium in Uranium Dioxide (MS Thesis). Univ. Calif.  
 Sung, P., 1967. Equilibrium Solubility and Diffusivity of Helium in Single-crystal Uranium Dioxide. Univ. Washington.  
 Talip, Z., Wiss, T., Di Marcello, V., Janssen, A., Colle, J.Y., Van Uffelen, P., Raison, P., Konings, R.J.M., 2014a. Thermal diffusion of helium in  $^{238}\text{Pu}$ -doped  $\text{UO}_2$ . J. Nucl. Mater. 445, 117–127. <http://dx.doi.org/10.1016/j.jnucmat.2013.10.066>.  
 Talip, Z., Wiss, T., Maugeri, E.A., Colle, J.Y., Raison, P.E., Gilibert, E., Ernstberger, M., Staicu, D., Konings, R.J.M., 2014b. Helium behaviour in stoichiometric and hyperstoichiometric  $\text{UO}_2$ . J. Eur. Ceram. Soc. 34, 1265–1277. <http://dx.doi.org/10.1016/j.jeurceramsoc.2013.11.032>.  
 Trocellier, P., Gosset, D., Simeone, D., Costantini, J.M., Deschanel, X., Roudil, D., Serruys, Y., Grynszpan, R., Saudé, S.E., Beauvy, M., 2003. Application of nuclear reaction geometry for  $^3\text{He}$  depth profiling in nuclear ceramics. Nucl. Instrum. Methods Phys. Res. Sect. B Beam Interact. Mater. Atoms 206, 1077–1082. [http://dx.doi.org/10.1016/S0168-583X\(03\)00914-5](http://dx.doi.org/10.1016/S0168-583X(03)00914-5).  
 Wiss, T., Hiernaut, J.P., Roudil, D., Colle, J.Y., Maugeri, E., Talip, Z., Janssen, A., Rondinella, V., Konings, R.J.M., Matzke, H.J., Weber, W.J., 2014. Evolution of spent nuclear fuel in dry storage conditions for millennia and beyond. J. Nucl. Mater. 451, 198–206. <http://dx.doi.org/10.1016/j.jnucmat.2014.03.055>.  
 Yakub, E., Ronchi, C., Staicu, D., 2010. Diffusion of helium in non-stoichiometric uranium dioxide. J. Nucl. Mater. 400, 189–195. <http://dx.doi.org/10.1016/j.jnucmat.2010.03.002>.  
 Yakub, E., Ronchi, C., Staicu, D., 2009. Computer simulation of defects formation and equilibrium in non-stoichiometric uranium dioxide. J. Nucl. Mater. 389, 119–126. <http://dx.doi.org/10.1016/j.jnucmat.2009.01.029>.